業績の種別	整理番号	著者名	表題	出典、巻、頁	発表年
原著	1	Arikawa-Hirasawa E, Le AH , Nishino I, Nonaka I, Ho NC , Francomano CA, Govindraj P, Hassell JR, Devaney JM , Spranger J, Stevenson RH, Iannaccone S, Dalakas MC, and Yamada Y.	Structural and functional mutations of the perlecan gene cause Schwartz-Jampel syndrome, with myotonic myopathy and chondrodysplasia.	Am. J. Hum. Gen., 70:1368-1375	2002
原著	2	Arikawa-Hirasawa E, Rossi SG, Rotundo RL, and Yamada Y.	Absence of acetylcholinesterase at the neuromuscular junctions of perlecan-null mice.	Nature Neuroscience, 5:119-123	2002
総説	3	Hassell J, Yamada Y, Arikawa-Hirasawa E.	Role of perlecan in skeletal development and diseases	Glycoconj J. 2002;19(4/5):263-267	2002
原著	4	Kobayashi H, Kruger R, Markopoulou K, Wszolek Z, Chase B, Taka H, Mineki R, Murayama K, Riess O, Mizuno Y, Hattori N.	Haploinsufficiency at the alpha-synuclein gene underlies phenotypic severity in familial Parkinson's disease.	Brain 126 (Pt 1):32-42	2002
原著	5	Ogawa T, Miyamae T, Murayama K, Okuyama K, Okayama T, Hagiwara M, Sakurada S, Morikawa T.	Synthesis and structure-activity relationships of an orally available and long-acting analgesic peptide, N(alpha)-amidino-Tyr-D-Arg-Phe-MebetaAla-OH (ADAMB).	J Med Chem. ;45(23):5081-9.	2002
原著	6	Sakurada S, Watanabe H, Hayashi T, Yuhki M, Fujimura T, Murayama K, Sakurada C, Sakurada T.	Endomorphin analogues containing D-Pro(2) discriminate different mu -opioid receptor mediated antinociception in mice.	Br J Pharmacol. 137(8):1143-1146.	2002
原著	7	Mineki R, Taka H, Fujimura T, Kikkawa M, Shindo N, Murayama K.	In situ alkylation with acrylamide for identification of cysteinyl residues in proteins during one- and two-dimensional sodium dodecyl sulphate-polyacrylamide gel electrophoresis.	Proteomics. 2(12):1672-81	2002
原著	8	Takai T, Mineki R, Nakazawa T, Takaoka M, Yasueda H, Murayama K, Okumura K, Ogawa H.	Maturation of the activities of recombinant mite allergens Der p 1 and Der f 1, and its implication in the blockade of proteolytic activity.	FEBS Lett. 531(2):265-72.	2002
原著	9	Hung KC, Wu HE, Mizoguchi H, Sakurada S, Okayama T, Fujimura T, Murayama K, Sakurada T, Fujimoto JM, Tseng LF.	D-pro(2)-endomorphin-1 and D-pro(2)-endomorphin-2, respectively, attenuate the antinociception induced by endomorphin-1 and endomorphin-2 given intrathecally in the mouse.	J Pharmacol Exp Ther.303(2) 874-879	2002
原著	10	Yamasaki H, Mineki R, Murayama K, Ito A, Aoki T.	Characterisation and expression of the Fasciola gigantica cathepsin L gene.	Int J Parasitol. 32(8):1031-42.	2002
原著	11	Kato A, Kawamata N, Tamayose K, Egashira M, Miura R, Fujimura T, Murayama K, Oshimi K.	Ancient ubiquitous protein 1 binds to the conserved membrane-proximal sequence of the cytoplasmic tail of the integrin alpha subunits that plays a crucial role in the inside-out signaling of alpha IIbbeta 3.	J Biol Chem. 277(32):28934-41	2002

原著	12	Sugie K, Yamamoto A, Murayama K, Oh SJ, Takahashi M, Mora M, Riggs JE, Colomer J, Iturriaga C, Meloni A, Lamperti C, Saitoh S, Byrne E, DiMauro S, Nonaka I, Hirano M, Nishino I.	Clinicopathological features of genetically confirmed Danon disease.	Neurology. Jun 25;58(12):1773-8.	2002
原著	13	Ishikawa H, Sugie K, Murayama K, Ito M, Minami N, Nishino I, Nonaka I.	Ullrich disease: collagen VI deficiency: EM suggests a new basis for muscular weakness.	Neurology. Sep 24;59(6):920-3.	2002
原著	14	Nishino I, Noguchi S, Murayama K, Driss A, Sugie K, Oya Y, Nagata T, Chida K, Takahashi T, Takusa Y, Ohi T, Nishimiya J, Sunohara N, Ciafaloni E, Kawai M, Aoki M, Nonaka I.	Distal myopathy with rimmed vacuoles is allelic to hereditary inclusion body myopathy.	Neurology. Dec10;59(11):1689-93.	2002
原著	15	Tateyama M, Aoki M, Nishino I, Hayashi YK, Sekiguchi S, Shiga Y, Takahashi T, Onodera Y, Haginoya K, Kobayashi K, Iinuma K, Nonaka I, Arahata K, Itoyoma Y.	Mutation in the caveolin-3 gene causes a peculiar form of distal myopathy.	Neurology 58: 323-5,	2002
原著	16	Isoda K, Nishikawa K, Kamezawa Y, Yoshida M, Kusuhara M, Moroi M, Tada N, and Ohsuzu F	Osteopontin plays an *important role* in the development of modial thickening and neointimal formation.	Circulation Res 91, 77-82, 2002	2002
原著	17	Maruyama H, Higuchi N, Nishikawa Y, Kameda S, Iino N, Kazawa JJ, Takahashi N, Sugawa M, Hanawa H, Tada N, Miyazaki J, and Gejyo F	High-level expression of naked DNA delivered to rat liver via tail vein injection.	J Gene Med 4, 333-341,	2002
原著	18	張 尚美、石川達也、埜中征哉、塚本東子、斎藤万里子、坂 京子、和田郁雄、杉江和馬、西野一三.	早期より鑿 形外科的問題を呈したメロシン陽 性型先天性筋ジストロフィ ーー Ullrich病との関連を含めて一.	脳と発達 35(2):159-164	2003
総説	19	Hayashi YK.	Membrane-repair machinery and muscular dystrophy.	Lancet. Sep 13;362(9387):843-4.	2003
原著	20	Winokur ST, Chen YW, Masny PS, Martin JH, Ehmsen JT, Tapscott SJ, Van Der Maarel SM, Hayashi Y, Flanigan KM.	Expression profiling of FHSD muscle supports a defect in specific stages of myogenic differentiation.	Hum Mol Genet. 12: 2895-2907,	2003
原著	21	Driss A, Noguchi S, Amouri R, Kefi M, Sasaki T, Sugie K, Souilem S, Hayashi YK, Shimizu N, Minoshima S, Kudou J, Hentati F, Nishino I.	Fukutin-related protein gene mutated in the original kindred limb-girdle MD 2I.	Neurology 60: 1341-1344,	2003

原著	22	Tagawa K, Ogawa M, Kawabe K, Yamanaka G, Matsumura T, Goto K, Nonaka I, Nishino I, Hayashi YK. Protein and gene analyses of dysferlinopathy in a large group of Japanese muscular dystrophy patients.	Protein and gene analyses of dysferlinopathy in a large group of Japanese muscular dystrophy patients.	J Neurol Sci 211: 23-28,	2003
原著	23	Taniguchi K, Kobayashi K, Saito K, Yamanouchi H, Ohnuma A, Hayashi YK, Manya H, Jin DK, Lee M, Parano E, Falsaperla R, Pavone P, Van Coster R, Talim B, Steinbrecher A, Straub V, Nishino I, Topaloglu H, Voit T, Endo T, Toda T.	Worldwide distribution and broader clinical spectrum of muscle-eye-brain disease.	Hum Mol Genet 12:527-534,	2003
原著	24	Ezaki J, Takeda-Ezaki M, Koike M, Ohsawa Y, Taka H, Mineki R, Murayama K, Uchiyama Y, Ueno T, Kominami K.	Characterization of Cln3P, the gene product resposibile for juvenile neuronal ceroid lipofuscinosis, as a lysosomal integral membrane glycoprotein.	J Neurochem. 87(5): 1296-308,	2003
原著	25	Yokono T, Mineki R, Taka H, Kotaniguchi H, Murayama K.	Improvement of automatic in-gel digestion by in situ alkylation of proteins.	J Bimo Tech. 14(3): 191-6,	2003
原著	26	Hanaguchi A, Suzuki E, Murayama K, Fujimura T, Hikita T, Iwabuchi K, Handa K, Withers DA, Masters SC, Fu H, Hakomori S.	A sphingosine-dependent protein kinase that specifically phosphorylates 14-3-3 (SDK1) is identified as the kinase domain of PKCdelta: a preliminary note.	Biochem Biophys Res Commun. 307(3): 589-94,	2003
原著	27	Hanaguchi A, Suzuki E, Murayama K, Fujimura T, Hikita T, Iwabuchi K, Handa K, Withers DA, Masters SC, Fu H, Hakomori S.	Sphingosine-dependent protein kinase-1, directed to 14-3-3 is identified as the kinase domain of protein kinase C delta.	J Biol Chem. 278(42): 41557-65,	2003
原著	28	Amino H, Osanai A, Miyadera H, Shinjyo N, Tomitsuka E, Taka H, Mineki R, Murayama K, Takamiya S, Aoki T, Miyoshi H, Sakamoto K, Kojima S, Kita K.	Isolation and characterization of the stage-specific cytochrome b small subunit (CybS) of Ascaris suum complex from the aerobic respiratory chain of larval mitochondoria.	Mol Biochem Parasitol. 128(2): 175-86,	2003
原著	29	Takamiya S, Yamasaki H, Hashimoto M, Taka H, Murayama K, Tagaya M, Aoki T.	Heterologous expression of Ascuris suum cytochrome b5 precursor protein: a histidine ξ tagged full-length presequence is correctly processed to transport the mature protein to the periplasma of Escherichia coli.	Arch Biochem Biophys. 413(2): 253-61,	2003
原著	30	Isoda K, Kamezawa Y, Ayaori M, Shiigai M, Kusuhara M, Tada N, and Ohsuzu F	Osteopontin transgenic mice fed a high cholesterol diet develop early fatty-streak lesions	Circulation 107, 679-681,	2003
総説	31	平澤恵理	Schwartz-Jampel症候群（軟骨異栄養症）とパールカン	Annual Review 神経2004	2004

原著	32	Yuasa K, Fukumoto S, Kamasaki Y, Yamada A, Fukumoto E, Kanaoka K, Saito K, Harada H, Arikawa-Hirasawa E, Miyagoe-Suzuki Y, Takeda S, Okamoto K, Kato Y, Fujiwara T.	Laminin alpha2 essential for odontoblast differentiation regulating dentin sialoprotein expression. J Biol Chem. 2003	J Biol Chem. 19;279(12):11402-7.	2004
原著	33	Vikramadithyan RK, Kako Y, Chen G, Hu Y, Arikawa-Hirasawa E, Yamada Y, Goldberg IJ.	Atherosclerosis in perlecan heterozygous mice.	J Lipid Res Oct;45(10):1806-12.	2004
総説	34	平澤恵理	パールカン の多様な機能の解明をめざして	Functional Glycomics No,4 20-23	2004
総説	35	平澤恵理	神経筋接合部におけるパールカンの役割	Glycoward NS-A03 ≈/Glycoforum(htt	2004
総説	36	平澤恵理	遺伝子改変マウスの解析から解明されるパールカンの神経筋機能への関与	『蛋白質核酸酵素』増刊号 神経糖鎖生物学 49:2425-2430	2004
原著	37	Goto K, Nishino I, Hayashi YK	Very low penetrance in 85 Japanese families with facioscapulohumeral muscular dystrophy 1	A. J Med Genet 41: E12, 2004	2004
原著	38	Ishikawa H, Sugie K, Murayama K, Awaya A, Suzuki Y, Noguchi S, Hayashi YK, Nonaka I, Nishino I.	Ullrich disease due to deficiency of collagen VI in the sarcolemma. Neurology 62: 620-623,	Neurology 62: 620-623,	2004
原著	39	Kim DS, Hayashi YK, Matsumoto H, Ogawa M, Noguchi S, Murakami N, Sakuta R, Mochizuki M, Michele DE, Campbell KP, Nonaka I, Nishino I.	POMT1 mutation results in defective glycosylation and loss of laminin-binding activity in alpha-DG.	Neurology 62: 1009-1011,	2004
原著	40	Noguchi S, Keira Y, Murayama K, Ogawa M, Fujita M, Kawahara G, Oya Y, Imazawa M, Goto Y, Hayashi YK, Nonaka I, Nishino I	Reduction of UDP-GlcNAc 2-epimerase/ManNAc kinase activity and sialylation in distal myopathy with rimmed vacuoles.	J Biol Chem 279: 11402-11407	2004
原著	41	Yamanaka G, Goto K, Ishihara T, Oya Y, Miyajima T, Hoshika A, Nishino I, Hayashi YK.	FSHD-like patients without 4q35 deletion.	J Neurol Sci 219: 89-93,	2004
原著	42	Matsumoto H, Noguchi S, Sugie K, Ogawa M, Murayama K, Hayashi YK, Nishino I	Subcellular localization of fukutin and fukutin-related protein in muscle cells.	J Biochem (Tokyo) 135 :709-712,	2004
原著	43	Kawabe K, Goto K, Nishino I, Angelini C, Hayashi YK	Dysferlin mutation analysis in a group of Italian patients with limb-girdle muscular dystrophy and Miyoshi myopathy.	Eur J Neurol 11: 657-661	2004

原著	44	Sugie K, Murayama K, Noguchi S, Murakami N, Mochizuki M, Hayashi YK, Nonaka I, Nishino I.	Two novel CAV3 gene mutations in Japanese families.	Neuromuscul Disord. 14: 810-814,	2004
総説	45	Hayashi, YK	Unusual clinical features associated with FSHD. In FSHD (Facioscapulohumeral Musucular Dystrophy) ~Clinical Medicine and Molecular Cell Biology~ (Eds)	Upadhyaya M, Cooper DN. BIOSIS Scientific Publishers, London and New York, p197-240	2004
原著	46	Nomiyama T, Igarashi Y, Taka H, Mineki R, Uchida T, Ogihara T, Choi JB, Uchino H, Tanaka Y, Maegawa H, Kashiwagi A, Murayama K, Kawamori R, Watada H	Reduction of insulin-stimulated glucose uptake by peroxynitrite is concurrent with tyrosine nitration of insulin receptor substrate-1.	Biochem Biophys Res Commun. 320(3):639-47,	2004
原著	47	Seko Y, Fujimura T, Taka H, Mineki R, Murayama K, Nagai R	Hypoxia followed by reoxygenation induces secretion of cyclophilin A from cultured rat cardiac myocytes.	Biochem Biophys Res Commun. 317(1):162-8,	2004
原著	48	Niki Y, Yamada H, Seki S, Kikuchi T, Takahashi H, Toyama Y, Fijikawa K, and Tada N:	contributes to chronic synovitis and cartilage destruction in human IL-1a transgenic mice。	J Immunol 172, 577-584,	2004
原著	49	Takahashi F, Takahashi K, Shimizu K, Cui R, Tada N, Takahashi H, Soma S, Yoshioka M, and Fukuchi Y:	Osteopontin is strongly expressed by alveolar macrophages in the lungs of acute respiratory distress syndrome.	Lung 182, 173-185,	2004
原著	50	Zhang D, Zhao J, Fujio K, Tada N, Sudo K, Tsurui H, Nakamura K, Yamamoto K, Nishimura H, Shirai T, and Hirose S	Dissection of the role of MHC class II A and E genes in autoimmune susceptibility in murine lupus models with intragenic recombination	Proc Natl Acad Sci USA 101, 13838-13843	2004
原著	51	Kaga N, Kazuno S, Taka H, Iwabuchi K, Murayama K.	Isolation and MSn characterization of molecular species of lactosylceramides using LC-ESI ion trap mass spectrometry.	Anal Biochem. 337(2):316-324,	2005
原著	52	Ichikawa N, Kasai S, Suzuki N, Nishi N, Oishi S, Fujii N, Kadoya Y, Hatori,K Mizuno Y, Nomizu M, and Arikawa-Hirasawa E	Identification of neurite outgrowth active sites on the laminin alpha4 chain G domain.	Biochemistry.	2005

III. 研究成果の刊行物・別刷

Am. J. Hum. Genet. 70:1368–1375, 2002

Report

Structural and Functional Mutations of the Perlecan Gene Cause Schwartz-Jampel Syndrome, with Myotonic Myopathy and Chondrodysplasia

Eri Arikawa-Hirasawa,[1,*] Alexander H. Le,[1] Ichizo Nishino,[3] Ikuya Nonaka,[3] Nicola C. Ho,[4,5] Clair A. Francomano,[4] Prasanthi Govindraj,[6] John R. Hassell,[6] Joseph M. Devaney,[7] Jürgen Spranger,[8] Roger E. Stevenson,[8] Susan Iannaccone,[9] Marinos C. Dalakas,[2] and Yoshihiko Yamada[1]

[1]Craniofacial Developmental Biology and Regeneration Branch, National Institute of Dental and Craniofacial Research, and [2]National Institute of Neuronal Disorders and Strokes, Bethesda; [3]Department of Ultrastructural Research, National Institute of Neuroscience, Tokyo; [4]Laboratory of Genetics, National Institute on Aging, and [5]Johns Hopkins Bayview Medical Center, Baltimore; [6]Shriners Hospital for Children, Tampa; [7]Children's National Medical Center, Washington; [8]Greenwood Genetic Center, Greenwood, SC; and [9]Texas Scottish Rite Hospital, Dallas

Perlecan, a large heparan sulfate proteoglycan, is a component of the basement membrane and other extracellular matrices and has been implicated in multiple biological functions. Mutations in the perlecan gene (*HSPG2*) cause two classes of skeletal disorders: the relatively mild Schwartz-Jampel syndrome (SJS) and severe neonatal lethal dyssegmental dysplasia, Silverman-Handmaker type (DDSH). SJS is an autosomal recessive skeletal dysplasia characterized by varying degrees of myotonia and chondrodysplasia, and patients with SJS survive. The molecular mechanism underlying the chondrodystrophic myotonia phenotype of SJS is unknown. In the present report, we identify five different mutations that resulted in various forms of perlecan in three unrelated patients with SJS. Heterozygous mutations in two patients with SJS either produced truncated perlecan that lacked domain V or significantly reduced levels of wild-type perlecan. The third patient had a homozygous 7-kb deletion that resulted in reduced amounts of nearly full-length perlecan. Unlike DDSH, the SJS mutations result in *different* forms of perlecan in reduced levels that are secreted to the extracellular matrix and are likely partially functional. These findings suggest that perlecan has an important role in neuromuscular function and cartilage formation, and they define the molecular basis involved in the difference in the phenotypic severity between DDSH and SJS.

Schwartz-Jampel syndrome (SJS [MIM 255800]) is a rare autosomal recessive skeletal dysplasia associated with myotonia (Aberfeld et al. 1965; Aberfeld et al. 1970). This disorder is characterized by short stature, osteochondrodysplasia, myotonia, and a characteristic face with a "fixed" facial expression, blepharophimosis, pursed lips, and, sometimes, low-set ears and myopia. Skeletal abnormalities include kyphoscoliosis, platyspondyly with coronal clefts in the vertebrae, metaphyseal and epiphyseal dysplasias, and joint contractures. Electromyography (EMG) shows persistent spontaneous activity, particularly in the face and thigh muscles, which tends to diminish at rest (Taylor et al. 1972; Jablecki and Schultz 1982). This spontaneous activity decreases with applications of curare in some patients, suggesting that the disorder is of neurogenic origin (Taylor et al. 1972; Fowler et al. 1974). Muscle biopsies show nonspecific myopathy (Fowler et al. 1974; Pascuzzi 1991). The clinical phenotype of SJS varies (Giedion et al. 1997). Mildly affected patients develop a moderate bone dysplasia in childhood. In more severely affected patients, a more obvious bone dysplasia, reminiscent of Kniest dysplasia, is present from infancy. Through linkage mapping and a positional candidate approach, Nicole et al. (2000) recently identified homozygous mutations in *HSPG2* in two families with SJS. The

Received November 28, 2001; accepted for publication February 22, 2002; electronically published April 8, 2002.

Address for correspondence and reprints: Dr. Yoshihiko Yamada, Building 30, Room 405, NIDCR, NIH, 30 Convent Drive, Bethesda, MD 20892. E-mail: yoshi.yamada@nih.gov

* Present affiliation: Department of Neurology, Juntendo University School of Medicine, Tokyo.

0002-9297/2002/7005-0029$15.00

mutations involved missense and splicing in *HSPG2*, but predicted mutant perlecan molecules have not been characterized.

Perlecan is a multifunctional proteoglycan present in all basement membranes and in cartilage (Iozzo et al. 1994; SundarRaj et al. 1995; French et al. 1999). The protein core is ~400 kD, with three covalently attached heparan sulfate chains at the N-terminus and another chain at the C-terminus (fig. 1*D*). Perlecan is implicated in cell growth and differentiation, through interactions with growth factors, cell surface receptors, and extracellular matrix molecules (Noonan et al. 1991; Aviezer et al. 1994; Dolan et al. 1997; Olsen 1999). The N-terminal domain, domain I, contains attachment sites for heparan sulfate chains and binds to growth factors (Iozzo 1994) and acetylcholinesterase (Peng et al. 1999). Domain IV binds basement membrane molecules, such as nidogen/entactin and type IV collagen (Hopf et al. 1999). Domain V binds cell surface receptors such as α-dystroglycan and integrin β1 (Brown et al. 1997; Friedrich et al. 1999).

The majority of mice with a homozygous null mutation in the perlecan gene (*Hspg2*) develop severe chondrodysplasia and die, just after birth, of respiratory failure (Arikawa-Hirasawa et al. 1999; Costell et al. 1999). Through comparison of skeletal abnormalities of human patients to the perlecan-null mice, we recently identified mutations in *HSPG2* in a lethal autosomal recessive disorder termed "dyssegmental dysplasia, Silverman-Handmaker type" (DDSH [MIM 224410])(Arikawa-Hirasawa et al. 2001). In DDSH, we found that truncated perlecan molecules were not secreted into the extracellular matrix, indicating that functional null mutations of the perlecan gene cause DDSH.

In the present report, we have identified, among three patients with SJS, five different mutations in *HSPG2* (GenBank accession number M852890), which result in different levels and forms of perlecan molecules. SJS perlecan molecules are secreted and partially functional, albeit in markedly reduced concentrations. Phenotypic differences in DDSH and SJS appear to reflect differences in the amount of functional perlecan in the matrix.

HSPG2 mutations in three patients with SJS were analyzed by RT-PCR and genomic sequencing (fig. 1). Patient 1 was an 8-year-old boy, born normally to healthy parents. At the age of 3 years, dysmorphic features were noted that became gradually prominent and consisted of tonic contraction of the facial muscles, micrognathia, low-set ears with folded helices, medial displacement of the outer canthi, narrow palpebral fissure, blepharophimosis, microstomia and pursing of the lips, high arched palate, cervical kyphosis, pes planus and valgus ankle formation, bowing of the leg bones, kyphoscoliosis, and lumbar lordosis. He had hypertrophic muscles and mild weakness of the quadriceps muscles. The creatinine kinase level was elevated (896 IU/liter); the EMG showed occasional myotonic discharges. Patient 2 was noted as having short stature and micromelia and was admitted to the hospital at 4 mo of age. Radiographs revealed square, flared ilia and short, bowed long bones. At 3 years of age, he showed thigh muscle hypertrophy and gastrocnemius muscle atrophy. Micrognathia, pursed lips, saddle nose, orbital hypertelorism, low-set ears, and high arched palate were noted. He showed a waddling gait, mild weakness of the quadriceps muscle, and percussion myotonia. EMG revealed myotonic and myopathic discharge. Necrotic and regenerating fibers were also found. Patient 3 was first reported as having micromelic chondrodysplasia (Stevenson 1982) but was reevaluated as having SJS in 2000 (Spranger et al. 2000). Micrognathia, a prominent philtrum, and bowed long bones were noted at age 3 mo. Radiographs revealed coronal clefts in the lumbar vertebrae, deficient ossification in the dorsal vertebrae, and squared, flared ilia. All long bones showed expansion of the metaphyses. At 4 years of age, facial movement became difficult because of stiffness, and the mouth opening was restricted. EMG showed pseudomyotonic discharge and rapid firing of single units in the brachioradial, deltoid, and medial gastrocnemius muscles.

Patient 1 had heterozygous mutations. Allele 1 had an A→G transition at the +4 position (donor site) of intron 56 (7374+4 A→G) that resulted in exon skipping of 56, whereas allele 2 of *HSPG2* contained a fusion of exons 60 and 61 that resulted in retention of intron 59 or intron 61 or in retention of both in the mutant transcripts. The exon fusion occurred at the precise acceptor and donor sites, probably by retrotransposition. The exon fusion mutation created aberrant transcripts. It also predicts the production of the wild-type transcript. A different primer set from exons 56 and 62, which was used to exclude a wild-type transcript from allele 1, confirmed the presence of the wild-type transcript, together with aberrant splicing transcripts produced by allele 2 (data not shown). The aberrant splicing from the two alleles is predicted to create premature termination codons. Patient 2 had a G→A transition at the last nucleotide of exon 64 (8544 G→A) in allele 1. This transition mutation did not change an amino acid but resulted in skipping of exon 64. Allele 2 has a 9-bp deletion (cagCTCCAG) at the acceptor junction of intron 66 and exon 67 in allele 2 (n−3 del9) that created abnormal splicing, including total or partial retention of intron 66 or skipping of exon 67. All aberrant splicing products are predicted to create premature termination codons. Patient 3 had a 7,108-bp homozygous deletion beginning at the 5′ portion of exon 96 (n+21 del7108) and extending well beyond the 3′ flanking sequence of *HSPG2*. This deletion created two aberrant transcripts; product 2 (derived from intron 95 retention) and product 1 (resulting from failure of splicing of both introns

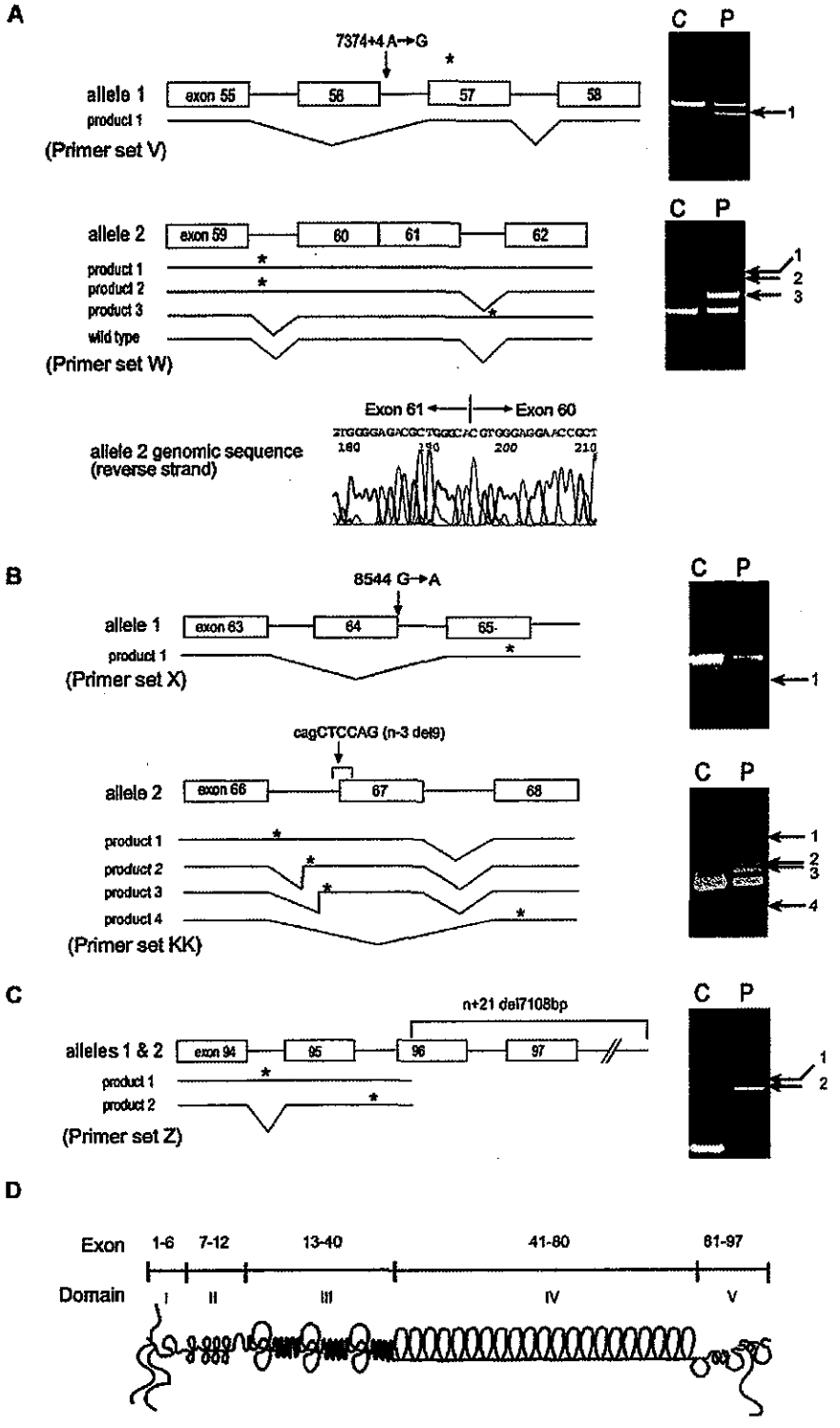
A
7374+4 A→G
allele 1
exon 55
58
57
58
product 1
(Primer set V)
C P
1
allele 2
exon 59
60
61
62
product 1
product 2
product 3
wild type
(Primer set W)
C P
1
2
3
Exon 61
Exon 60
allele 2 genomic sequence
(reverse strand)
180
200
210
B
8544 G→A
allele 1
exon 63
64
65
product 1
(Primer set X)
C P
1
cagCTCCAG (n-3 del9)
allele 2
exon 66
67
68
product 1
product 2
product 3
product 4
(Primer set KK)
C P
1
2
3
4
C
n+21 del7108bp
alleles 1 & 2
exon 94
95
96
97
product 1
product 2
(Primer set Z)
C P
1
2
D
Exon
1-6
7-12
13-40
41-80
81-97
Domain
I
II
III
IV
V

94 and 95) are predicted to produce truncated proteins missing ~35 and ~64 amino acids from the C-terminal, respectively.

We next examined the expression of perlecan in muscles from patients 1 and 2 by immunostaining with domain-specific antiperlecan antibodies (fig. 2). Perlecan was localized in the control tissue in the basal lamina of the muscle fibers and in the capillaries. Similar but weaker staining for domains III–V was observed in the muscles of patient 1 (fig. 2*A*), consistent with the presence of the wild-type transcript. We observed a similar immunostaining of fibroblasts from patient 1 (data not shown). In patient 2, domains III and IV were present in the muscle at a reduced level compared with the control specimen, but domain V was missing, suggesting a defect in domain V (fig. 1). The aberrant splicing transcripts from both alleles of patient 2 are predicted to produce truncated perlecan molecules that lack the C-terminal part of domain IV and all of domain V. Thus, the immunostaining results agree with the predicted truncated proteins. We examined immunostaining of cultured fibroblasts from patient 3, because no tissue from a muscle biopsy of this patient was available. In patient 3 fibroblasts, domains III–V were present in the matrix but with significantly less staining than in the control specimen (fig. 2*B*). Because a 7-kb homozygous deletion in *HSPG2* of patient 3 eliminates only 35–64 amino acids in the C-terminal domain V, these results are consistent with the genetic analysis.

Perlecan secretion from fibroblasts of patients 1 and 3 was next examined using western blot analysis (fig. 3). After removal of heparan sulfate chains by heparitinase treatment, conditioned media from normal fibroblasts showed a protein core of perlecan that was ~400-kD. Patient 1 fibroblasts secreted a 400-kD protein core in significantly reduced amounts compared with the wild-type protein core, supporting the presence of the wild-type transcript. The fibroblasts also secreted a smaller immunostainable band of ~150 kD, which may be a degraded product as is seen in the control fibroblasts. Conditioned media from patient 3 fibroblasts contained a 400-kD protein, which is predicted to lack ~35–64 C-terminal amino acids. As with patient 1, the amount of perlecan secreted was significantly reduced compared with that of the control.

In the patients we studied for the present report, partial functional mutations in *HSPG2* caused SJS, which is characterized by myotonia associated with a chondrodysplasia phenotype. Five mutations were identified in three patients with SJS, with one homozygous and four heterozygous mutations. These mutations produce different forms of the perlecan molecule. In patient 1, the staining of domain V in muscles was present at levels similar to those of other domains, and western blot analysis showed no obviously truncated molecules. These results suggest that, in patient 1, only the normal protein is secreted in the matrix, although in a reduced amount. The predicted truncated molecules were likely unstable because of proteolytic degradation or instability of the mutant transcripts. In patient 2, mutant perlecan lacking domain V was produced with reduced levels, compared with the control. In patient 3, a 7-kb homozygous deletion near the end of *HSPG2* produces a nearly full-length perlecan molecule at reduced levels.

Figure 1 Mutation analysis and schematic diagram of perlecan. *A*, Results of RT-PCR RNA from patient 1 fibroblasts, using primer sets V and W and analyzed on 1% agarose gels as described elsewhere (Arikawa-Hirasawa et al. 2001). Sequencing revealed that product 1 from allele 1 was missing the entire exon 56 sequence and that products 1, 2, and 3 from allele 2 retained intron sequences. Product 3 of allele 2 contains the sequence of intron 61, whereas products 1 and 2 contain either both introns 59 and 61 or intron 59, respectively. Exon 56 skipping in allele 1 causes frameshift and is predicted to produce a premature termination codon in exon 57. The intron 59 retention of products 1 and 2 from allele 2 is predicted to produce a premature termination codon within intron 59, and the intron 61 retention of product 3 is predicted a termination codon within intron 61. Genomic sequencing identified heterozygous mutations in an A→G transition at the +4 position (donor site) of intron 56 (7374+4 A→G) in allele 1. Allele 2 showed a complete loss of intron 60, resulting in fusion of exons 60 and 61 in the perlecan gene. The exon fusion mutation created aberrant transcripts, products 1, 2, and 3, but is also predicted to produce the wild-type product. Since primer set W does not distinguish the wild-type product derived from alleles 1 or 2, we used a primer set from exons 56 and 62 to exclude a wild-type transcript from allele 1, in which exon 56 is missing and confirmed the presence of the wild-type transcript together with aberrant splicing transcripts produced by allele 2 (data not shown). *B*, Patient 2. RT-PCR was performed with RNA from skeletal muscle tissues of patient 2, using primer sets X and KK. Sequencing of product 1 with primers X revealed exon 64 skipping, and products 1, 2, and 3 with primers KK contained total or partial retention of intron 66. Product 4 with primers KK showed exon 67 skipping. Genomic sequencing revealed a heterozygous mutation in a G to A transition at the donor site of exon 64 (8564 G→A) in allele 1 and a 9-bp deletion (cagCTCCAG) at the acceptor junction of intron 66 and exon 67 in allele 2 (n-3 del9). *C*, Patient 3. RT-PCR was performed with RNA from patient 3 fibroblasts using primer set Z. Product 1 contained sequences including introns 94 and 95. Product 2, a major product, contained intron 95. Sequencing of the genomic PCR product revealed a 7,108-bp deletion beginning at the 5′ portion of exon 96 and extending to the 3′ flanking sequence of *HSPG2*. The deletion results in aberrant splicing, including exon skipping and intron retention. Asterisk (*) indicates a premature termination codon. Arrows indicate abnormally sized RT-PCR products. *D*, Schematic diagram of perlecan and its exon and domain structure. Primer sequences for RT-PCR are as follows: V (forward, ATCACGGTCACAGTAACTGGGACC; reverse, CCTGCACCGTTACTGACGTG); KK (forward, ATGGCACAAGCGTGGAGGAAACC; reverse, AGGCTTCTTGCTCAGGGCCTGG); W (forward, ATCCAGCAGCGCCTTAGTGG; reverse, CATGCCCATCAGAATTGAGTCAT); X (forward, CTCAACAACATCGATGCCCTGGAG; reverse, CTCCAGCCCAGGACCCATTCCT); and Z (forward, AGGCAAGGACTTCATCAGCCTCGGG; reverse, TCGACTTGGATGGAACCTCTGCGG).

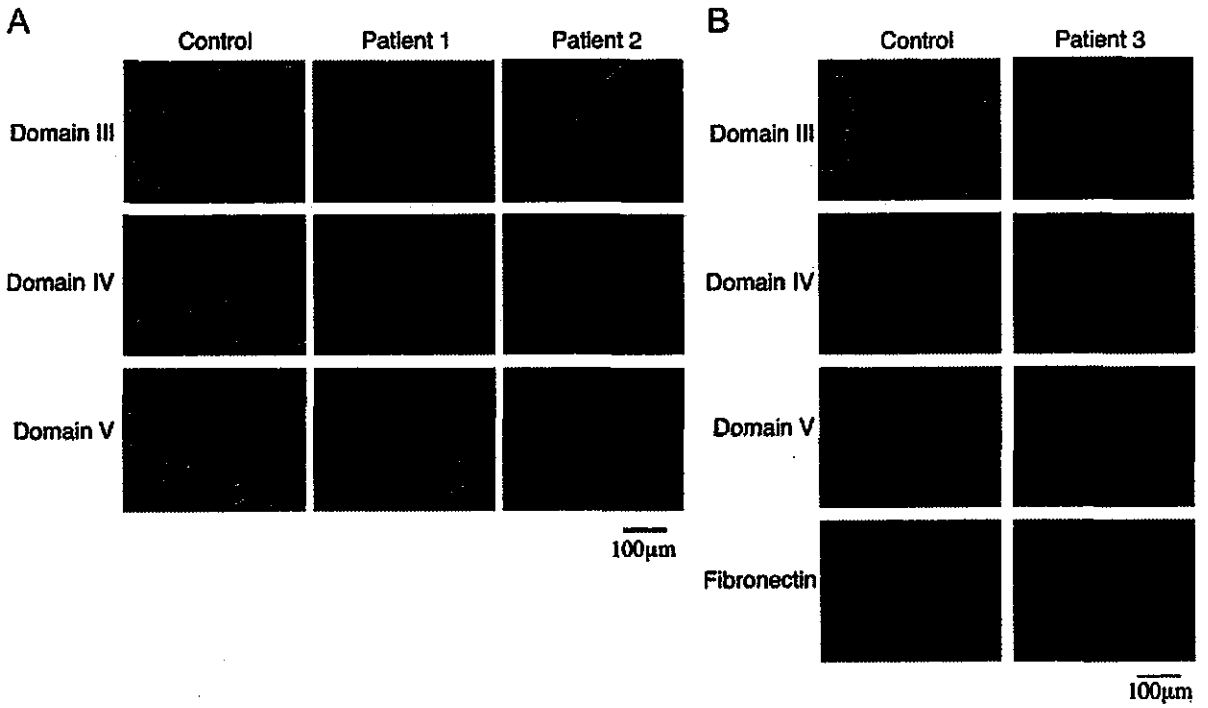

Figure 2 Immunostaining of perlecan in muscle tissues and cultured fibroblasts. *A*, Muscle tissue from patients 1 and 2 and from an unaffected control subject, stained with domain-specific anti-perlecan antibodies as described elsewhere (Arikawa-Hirasawa et al. 2001, 2002). In patient 1, antibodies to domains III–V stained the basal lamina of the muscle, whereas, in patient 2, domain V staining was absent. The staining in muscle tissue of patient 1 is significantly reduced. *B*, Cultured fibroblasts from patient 3 stained with domain-specific anti-perlecan antibodies and with anti-fibronectin polyclonal antibodies. Domains III–V stained the extracellular matrix at significantly reduced levels compared to control fibroblasts, whereas fibronectin stained strongly in both.

In patients with DDSH, we did not detect perlecan in the cartilage matrix or in the matrix from cultured fibroblasts (Arikawa-Hirasawa et al. 2001); however, in contrast to results in patients with DDSH, we found that mutant perlecan molecules or reduced amounts of wild-type perlecan are secreted and localized in the matrix of tissues from patients with SJS. In DDSH, there is mucoid degeneration of the resting cartilage, as well as abnormal chondrocyte columnar structures and defective mineralization of the growth plate. Although only limited information is available about the histology of cartilage from patients with SJS, there is a report that indicates poor chondrocyte columnar organization in epiphyseal cartilage of one patient with SJS (Aberfeld et al. 1965). The SJS perlecan molecules in the matrix are partially functional, which results in a milder chondrodysplasia phenotype than that of DDSH. In normal growth-plate cartilage, perlecan likely strengthens the extracellular matrix structure by interacting with other molecules. Impaired cartilage matrix resulting from partially functional perlecan may contribute to the skeletal abnormalities in patients with SJS. Patients 2 and 3 showed obvious micromelia in their early infancy, but patient 1 showed a chondrodysplasia phenotype that was not obvious until the patient was 3–4 years of age. This difference may result from the fact that only patient 1 produces the normal perlecan molecule. Because the truncated perlecan molecules of patients 2 and 3 are defective in domain V, the C-terminal domain V may be responsible for the early onset of skeletal abnormalities. It is conceivable that domain V plays a role in matrix-cell interaction through its binding to a chondrocyte receptor, such as integrin, providing stable formation of the cartilage matrix structure. Some of the skeletal abnormalities, such as scoliosis and hip degeneration, in patients with SJS could be caused, in part, by the myotonia in SJS.

Another characteristic of the SJS phenotype involves abnormal neuromuscular functions. A unique set of molecules—including acetylcholine esterase (AChE), acetylcholine receptor (AChR), and perlecan—cluster at sites of nerve-muscle contact to form the neuromuscular junction (NMJ), where muscle contraction is initiated. The collagen-tailed form of AChE is highly expressed in innervated regions of skeletal muscle fibers and is attached

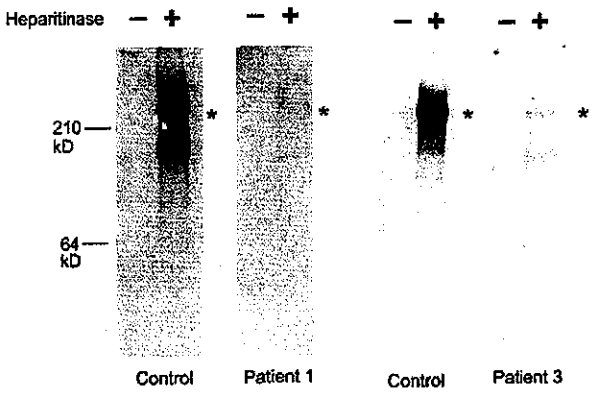

Figure 3 Perlecan secreted by cultured fibroblasts in patients 1 and 3. Media from cultured normal or patient fibroblasts were concentrated, were then adjusted to contain 0.35g CsCl/g of 4M guanidine, and were centrifuged for 72 h at 40,000 RPM in a 50-Ti rotor at 12°C. A proteoglycan-containing fraction was pooled, concentrated, and digested with 0.1 mU heparitinase and 0.25 mU chondroitinase ABC (Seikagaku). Digested and undigested samples were electrophoresed in 3%–8% polyacrylamide tris-acetate gels, were transferred to nitrocellulose, and were blotted with polyclonal antibodies to the perlecan protein core. In patient 1, a perlecan protein core of ~400 kD was detected after heparitinase digestion, but the amount was reduced significantly, correlating with the reduced amount of the wild-type perlecan transcript. Heparitinase treatment is necessary for the blotting, because perlecan-containing heparan sulfate chains do not transfer well onto a membrane because of the negatively charged heparan sulfate chains. As with patient 1, patient 3 fibroblasts secreted the 400-kD perlecan core protein in much more reduced amounts than did the control cells. The truncated perlecan in patient 3 is missing only ~35–64 amino acids of the most C-terminal part of domain V, suggesting the mutant perlecan to be almost the same size as the wild-type perlecan. Asterisks (*) indicate positions of the ~400-kD protein core.

to the synaptic basal lamina (Massoulie et al. 1993). In vertebrate skeletal muscle, ACh acts as a neurotransmitter, and AChE is responsible for rapid termination of neurotransmission, by hydrolyzing ACh at the synapse. In vitro studies show that perlecan binds to AChE, suggesting that perlecan is an acceptor site for AChE at the NMJ (Peng et al. 1999). How do the perlecan defects cause the myotonic phenotype of SJS? Unlike the mutations in perlecan-null mice and patients with DDSH, mutations in the patients with SJS produce partially functional perlecan molecules, which are present in the basal lamina of the muscle. We recently demonstrated, using perlecan-null mice, that clustering molecules, such as AChR and agrin, were present at the NMJ but that AChE was completely absent, indicating that perlecan is a key molecule for localizing AChE at the synapse (Arikawa-Hirasawa et al. 2002). The reduced amounts of either truncated or normal perlecan molecules may result in reduced clustering of AChE at the SJS NMJ, which would likely cause a greater concentration of ACh. This would stimulate AChR activity and thus cause myotonia. This mechanism is different from that of other hereditary myotonias, which are caused by defects in muscle membrane proteins involved in the sodium channel. Mutations in the gene *COLQ* for a collagenlike subunit of AChE were reported to cause end-plate AChE deficiency (EAD), which is characterized by a congenital myasthenic syndrome associated with weakness and fatigability on exertion (Donger et al. 1998; Ohno et al. 1998). In this disorder, AChE cannot form a heteromeric asymmetric complex with COLQ, and it is therefore inactive for enzymatic activity. The difference in the phenotype of SJS and EAD may result from the difference of AChE activity. In SJS, normal AChE is produced and clustered at the NMJ—although in reduced amounts—whereas, in EAD, there is no active AChE. Without any AChE activity, there is no recycling of ACh, which may lead to excessive depletion of ACh that, in turn, causes a myasthenic syndrome. Curare, which blocks transmission, can abolish persistent spontaneous activity of the electromyography in patients with SJS but not in other myotonias that result from defects in muscle membrane proteins (Taylor et al. 1972). This curare effect is in concordance with our proposed mechanism by which defects in perlecan cause SJS myotonia. However, in some patients with SJS, curare does not arrest the spontaneous activity (Spaans et al. 1990). This may result from a secondary defect in muscle membranes caused by mutations in the perlecan gene. Chronic impairment of NMJ activity due to increased levels of ACh is known to cause degeneration of the folds of the NMJ (Engel et al. 1977; Salpeter et al. 1979). Less stable synaptic basal lamina structures may be formed because of the significant reduction of wild-type perlecan or because of mutant perlecan defective in domain V, which leads to reduced expression of clustering molecules.

Recently, Spranger et al. reported that several other skeletal disorders previously identified as chondrodysplasias, such as kyphomelic chondrodysplasia, micromelic chondrodysplasia, and Burton disease, can be reclassified, on the basis of clinical examination, as SJS (Spranger et al. 2000). One of the patients with SJS in the present report was originally classified as having micromelic chondrodysplasia. Thus, the clinical phenotype of SJS encompasses a broad spectrum. Molecular and biochemical analysis of perlecan from these patients should provide more insight into phenotype-genotype correlations and functional domains of perlecan.

Acknowledgments

We thank Drs. C. McDonald, W. Fowler, E. Hoffman, C. Schwartz, and W. Wilcox, for helpful discussions, and Drs. R. Rotundo and H. Kleinman, for comments on the manuscript. We also thank H. Grant, for editorial help, and R. Granger,

for technical help. This work was supported by National Institutes of Health intramural funds to Y.Y., C.F., and M.D. and by grants to J.R.H. from the Shriners of North America. A.H.L. is a Howard Hughes Medical Institute–National Institutes Research Fellow.

Electronic-Database Information

Accession numbers and URLs for data in this article are as follows:

GenBank, http://www.ncbi.nlm.nih.gov/GenBank/ (for the sequence of *HSPG2* cDNA [accession number M852890] and for *HSPG2*-containing human chromosome 1 working draft sequence segment [accession number NT_004576])
Online Mendelian Inheritance in Man (OMIM), http://www.ncbi..nih.gov/Omin/ (for SJS [MIM 255800] and DDSH [MIM 224410])

References

Aberfeld DC, Hinterbuchner LP, Schneider M (1965) Myotonia, dwarfism, diffuse bone disease and unusual ocular and facial abnormalities (a new syndrome). Brain 88:313–322

Aberfeld DC, Namba T, Vye MV, Grob D (1970) Chondrodystrophic myotonia: report of two cases—myotonia, dwarfism, diffuse bone disease, and unusual ocular and facial abnormalities. Arch Neurol 22:455–462

Arikawa-Hirasawa E, Rossi SG, Rotundo RL, Yamada Y (2002) Absence of acetylcholinesterase at the neuromuscular junctions of perlecan-null mice. Nat Neurosci 5:119–123

Arikawa-Hirasawa E, Watanabe H, Takami H, Hassell JR, Yamada Y (1999) Perlecan is essential for cartilage and cephalic development. Nat Genet 23:354–358

Arikawa-Hirasawa E, Wilcox WR, Le AH, Silverman N, Govindraj P, Hassell JR, Yamada Y (2001) Dyssegmental dysplasia, Silverman-Handmaker type, is caused by functional null mutations of the perlecan gene. Nat Genet 27:431–434

Aviezer D, Hecht D, Safran M, Eisinger M, David G, Yayon A (1994) Perlecan, basal lamina proteoglycan, promotes basic fibroblast growth factor-receptor binding, mitogenesis, and angiogenesis. Cell 79:1005–1013

Brown JC, Sasaki T, Gohring W, Yamada Y, Timpl R (1997) The C-terminal domain V of perlecan promotes β1 integrin-mediated cell adhesion, binds heparin, nidogen and fibulin-2 and can be modified by glycosaminoglycans. Eur J Biochem 250:39–46

Costell M, Gustafsson E, Aszodi A, Morgelin M, Bloch W, Hunziker E, Addicks K, Timpl R, Fassler R (1999) Perlecan maintains the integrity of cartilage and some basement membranes. J Cell Biol 147:1109–1122

Dolan M, Horchar T, Rigatti B, Hassell JR (1997) Identification of sites in domain I of perlecan that regulate heparan sulfate synthesis. J Biol Chem 272:4316–4322

Donger C, Krejci E, Serradell AP, Eymard B, Bon S, Nicole S, Chateau D, Gary F, Fardeau M, Massoulie J, Guicheney P (1998) Mutation in the human acetylcholinesterase-associated collagen gene, COLQ, is responsible for congenital myasthenic syndrome with end-plate acetylcholinesterase deficiency (type Ic). Am J Hum Genet 63:967–975

Engel AG, Lambert EH, Gomez MR (1977) A new myasthenic syndrome with end-plate acetylcholinesterase deficiency, small nerve terminals, and reduced acetylcholine release. Ann Neurol 1:315–330

Fowler WM Jr, Layzer RB, Taylor RG, Eberle ED, Sims GE, Munsat TL, Philippart M, Wilson BW (1974) The Schwartz-Jampel syndrome: its clinical, physiological and histological expressions. J Neurol Sci 22:127–146

French MM, Smith SE, Akanbi K, Sanford T, Hecht J, Farach-Carson MC, Carson DD (1999) Expression of the heparan sulfate proteoglycan, perlecan, during mouse embryogenesis and perlecan chondrogenic activity in vitro. J Cell Biol 145: 1103–1115

Friedrich MV, Gohring W, Morgelin M, Brancaccio A, David G, Timpl R (1999) Structural basis of glycosaminoglycan modification and of heterotypic interactions of perlecan domain V. J Mol Biol 294:259–270

Giedion A, Boltshauser E, Briner J, Eich G, Exner G, Fendel H, Kaufmann L, Steinmann B, Spranger J, Superti-Furga A (1997) Heterogeneity in Schwartz-Jampel chondrodystrophic myotonia. Eur J Pediatr 156:214–223

Hopf M, Gohring W, Kohfeldt E, Yamada Y, Timpl R (1999) Recombinant domain IV of perlecan binds to nidogens, laminin-nidogen complex, fibronectin, fibulin-2 and heparin. Eur J Biochem 259:917–925

Iozzo RV (1994) Perlecan: a gem of a proteoglycan. Matrix Biol 14:203–208

Iozzo RV, Cohen IR, Grassel S, Murdoch AD (1994) The biology of perlecan: the multifaceted heparan sulphate proteoglycan of basement membranes and pericellular matrices. Biochem J 302:625–639

Jablecki C, Schultz P (1982) Single muscle fiber recordings in the Schwartz-Jampel syndrome. Muscle Nerve Suppl 5:S64–S69

Massoulie J, Pezzementi L, Bon S, Krejci E, Vallette FM (1993) Molecular and cellular biology of cholinesterases. Prog Neurobiol 41:31–91

Nicole S, Davoine CS, Topaloglu H, Cattolico L, Barral D, Beighton P, Hamida CB, Hammouda H, Cruaud C, White PS, Samson D, Urtizberea JA, Lehmann-Horn F, Weissenbach J, Hentati F, Fontaine B (2000) Perlecan, the major proteoglycan of basement membranes, is altered in patients with Schwartz-Jampel syndrome (chondrodystrophic myotonia). Nat Genet 26:480–483

Noonan DM, Fulle A, Valente P, Cai S, Horigan E, Sasaki M, Yamada Y, Hassell JR (1991) The complete sequence of perlecan, a basement membrane heparan sulfate proteoglycan, reveals extensive similarity with laminin A chain, low density lipoprotein-receptor, and the neural cell adhesion molecule. J Biol Chem 266:22939–22947

Ohno K, Brengman J, Tsujino A, Engel AG (1998) Human endplate acetylcholinesterase deficiency caused by mutations in the collagen-like tail subunit (ColQ) of the asymmetric enzyme. Proc Natl Acad Sci USA 95:9654–9659

Olsen BR (1999) Life without perlecan has its problems. J Cell Biol 147:909–912

Pascuzzi RM (1991) Schwartz-Jampel syndrome. Semin Neurol 11:267–273

Peng HB, Xie H, Rossi SG, Rotundo RL (1999) Acetylcholinesterase clustering at the neuromuscular junction involves perlecan and dystroglycan. J Cell Biol 145:911–921

Salpeter MM, Kasprzak H, Feng H, Fertuck H (1979) Endplates after esterase inactivation in vivo: correlation between esterase concentration, functional response and fine structure. J Neurocytol 8:95–115

Spaans F, Theunissen P, Reekers AD, Smit L, Veldman H (1990) Schwartz-Jampel syndrome. I. Clinical, electromyographic, and histologic studies. Muscle Nerve 13:516–527

Spranger J, Hall BD, Hane B, Srivastava A, Stevenson RE (2000) Spectrum of Schwartz-Jampel syndrome includes micromelic chondrodysplasia, kyphomelic dysplasia, and Burton disease. Am J Med Genet 94:287–295

Stevenson RE (1982) Micromelic chondrodysplasia. Proc Greenwood Genet Ctr 1:52–56

SundarRaj N, Fite D, Ledbetter S, Chakravarti S, Hassell JR (1995) Perlecan is a component of cartilage matrix and promotes chondrocyte attachment. J Cell Sci 108: 2663–2672

Taylor RG, Layzer RB, Davis HS, Fowler WM Jr (1972) Continuous muscle fiber activity in the Schwartz-Jampel syndrome. Electroencephalogr Clin Neurophysiol 33:497–509

Absence of acetylcholinesterase at the neuromuscular junctions of perlecan-null mice

Eri Arikawa-Hirasawa[1,2], Susana G. Rossi[3], Richard L. Rotundo[3] and Yoshihiko Yamada[1]

[1] *Craniofacial Developmental Biology and Regeneration Branch, National Institute of Dental and Craniofacial Research, National Institutes of Health, 9000 Rockville Pike, Bethesda, Maryland, 20892 USA*

[2] *Present address: Department of Neurology, Juntendo University Medical School, 2-1-1 Hongo, Bunkyo-ku, Tokyo, Japan*

[3] *Department of Cell Biology and Anatomy and Neuroscience Program, University of Miami School of Medicine, 1600 NW 10th Avenue, Miami, Florida, 33136 USA*

Correspondence should be addressed to R.L.R. (rrotundo@miami.edu) or Y.Y. (Yoski.yamada@nih.gov)

Published online: 22 January 2002, DOI:10.1038/nn801

The collagen-tailed form of acetylcholinesterase (AChE) is concentrated at the vertebrate neuromuscular junction (NMJ), where it is responsible for rapidly terminating neurotransmission. This unique oligomeric form of AChE, consisting of three tetramers covalently attached to a collagen-like tail, is more highly expressed in innervated regions of skeletal muscle fibers, where it is externalized and attached to the synaptic basal lamina interposed between the nerve terminal and the receptor-rich postsynaptic membrane. Although it is clear that the enzyme is preferentially synthesized in regions of muscle contacted by the motoneuron, the molecular events underlying its localization to the NMJ are not known. Here we show that perlecan, a multifunctional heparan sulfate proteoglycan concentrated at the NMJ, is the unique acceptor molecule for collagen-tailed AChE at sites of nerve–muscle contact and is the principal mechanism for localizing AChE to the synaptic basal lamina.

Acetylcholinesterase (AChE) was the first molecular component identified at sites of nerve–muscle contact[1] and has long been used as a marker for the development and organization of the neuromuscular junction (NMJ)[2,3]. The collagen-tailed form of AChE was first described in 1969[4] and later shown to be preferentially expressed in innervated regions of muscle[5] and to interact with the extracellular matrix[6]. These interactions are specific for the collagen-like tail (ColQ), which is capable of electrostatic binding to a variety of proteoglycans[7,8] as well as to purified heparin[9]. The collagen-like tail is absolutely necessary for the appearance of AChE at the NMJ[10], and mutations of the gene encoding ColQ in humans lead to a severe congenital myasthenia[11,12]. Most, if not all, of the AChE localized at the NMJ is associated with the synaptic basal lamina[13], to which it becomes covalently attached once externalized[14,15]. The expression of AChE in innervated regions of muscle is due to local accumulation of its transcripts[16–18], and the translated enzyme is then transported to the overlying region of the plasma membrane[19]. The mechanisms whereby AChE is localized and retained at sites of nerve–muscle contact are not known.

Perlecan is another component of the vertebrate NMJ that is concentrated on the synaptic basal lamina and at clusters on tissue-cultured myotubes, where it co-localizes with the nicotinic acetylcholine receptors (AChR)[20–22]. Perlecan is a complex, multifunctional heparan sulfate proteoglycan expressed in many vertebrate tissues, where it has an important role in the formation of extracellular matrices and in cell–cell interactions both during development and differentiation and in the mature organism[23]. In mice, deletion of the gene encoding perlecan gene (*Hspg2*) by homologous recombination is lethal, with the majority of affected mice dying at birth from respiratory failure[24,25]. Recent studies have shown that AChE can bind directly to perlecan, both *in vitro* and on the surface of muscle cells in tissue culture, and that perlecan, binding to dystroglycan, may be responsible for localizing AChE to sites of nerve–muscle contact[26]. The observations that the purified collagen-tailed form of AChE from one species can be 'transplanted' onto the NMJ of another[26,27] indicated that there might be specific binding sites for this synaptic component at sites of nerve–muscle contact. The evidence that AChE could bind to perlecan, together with their co-localization both in culture and in adult muscle, indicated that perlecan might be part of the binding site for collagen-tailed AChE at the NMJ. To test this hypothesis, we studied the innervation of skeletal muscle fibers isolated from mice heterozygous or null for *Hspg2*. Our results show that, in the absence of perlecan, AChE does not localize and accumulate at the NMJ.

Results

Because perlecan-null mice die shortly after birth, most of our studies were carried out on embryos at embryonic day 18.5 (E18.5). These embryos were smaller than their homozygous wild-type or heterozygous littermate controls. Details of their phenotype have been recently described[24]. Examination of the skeletal muscle showed no evidence of gross abnormalities upon dissection. Staining of frozen sections of limb muscles showed that they developed normally, with the same density of muscle

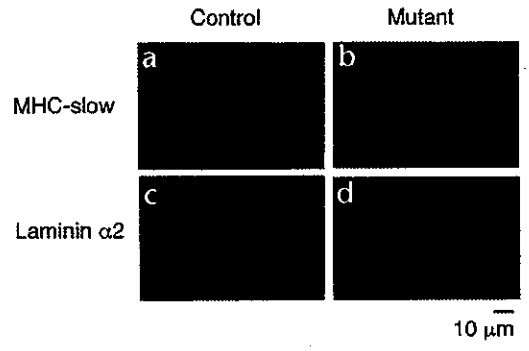

Fig. 1. Muscle development is normal in perlecan-null mice. (a,b) Muscle development and differentiation in normal heterozygous and perlecan-null mice were examined in transverse sections of frozen E18.5 limb muscles immunostained for myosin heavy-chain isoforms (MHC) using antibodies against the adult forms of slow and fast MHC. The size and density of muscle fibers in sections from normal heterozygous (+/–) and mutant (–/–) mice were similar. Immunofluorescence staining for slow MHC showed no significant differences in the distribution of slow fibers between heterozygous control (a) and mutant (b) embryonic muscles. Similar staining patterns were observed for fast MHC in heterozygous and perlecan-null mice (data not shown). These results suggest that muscle development occurs normally in the absence of perlecan, at least until birth. (c,d) Expression of the laminin α2 chain in E18.5 heterozygous (c) and perlecan-null muscle (d) was compared by immunostaining. The laminin α2 chain is localized in the extracellular matrix surrounding the muscles in both normal and mutant mice, indicating that a basement membrane is present in perlecan-null muscle.

fibers in heterozygous control and perlecan-null muscles (Fig. 1). To determine whether the muscle fibers were differentiating normally, frozen sections of limb muscle were stained with antibodies against fiber type–specific myosin heavy chains (MHC). Immunofluorescence localization of slow-fiber-type MHC showed an identical distribution of fiber types in normal and mutant mice (Fig. 1a and b), as did antibodies against the fast type MHC (data not shown), indicating that the muscles developed and differentiated normally.

Skeletal muscle fibers are surrounded by an extracellular matrix whose principal constituents include collagen type IV, fibronectin and laminin[28–30]. The laminin α2 chain is expressed in the perinatal muscle basement membrane during normal development[31]. Staining of E18.5 muscle with antibodies against the laminin α2 chain showed that the basal lamina surrounding each fiber also seemed to develop normally, as indicated by the similar distribution of the laminin α2 chains in both groups of mice (Fig. 1c and d). Thus, at least at the light-microscopic level, the extracellular matrix does not require perlecan in order to assemble around the fibers.

To examine the formation of the NMJ, we labeled tissue samples with a combination of antibodies against neurofilament H and synaptophysin to determine the distribution of nerve fibers and terminals. Whole mounts of embryonic diaphragms from normal (wild-type) and perlecan-null mice showed similar distributions of neurofilament H and synaptophysin that co-localized with AChR (Fig. 2a and b), indicating that the pattern of nerve branching was similar and suggesting that similar numbers of nerve terminals were present in each case. Higher-power views (Fig. 2a and b, inserts), as well as stained cross-sections of muscle (data not shown), showed that the synaptophysin labeling co-distributed with AChR labeled with the specific ligand fluorescent α-bungarotoxin (α-Btx), indicating that the nerve terminals remained closely associated with the NMJ and did not extend beyond the synapse. Examination of teased muscle fibers labeled with fluorescent α-Btx to reveal the NMJs (Fig. 2c and d) showed that all fibers were innervated in both wild-type and mutant muscles. To quantify the effects of perlecan absence, we measured the surface areas of the NMJs and total relative fluorescence of labeled AChR and AChE on 17 muscle fibers from 2 wild-type and 2 perlecan-null mice (Table 1). The area occupied by the AChR at perlecan-null NMJs was ~30% greater than at wild-type NMJs, although the difference was just statistically significant at the 0.05 level (paired Student's t-test, $t = 2.37$, $p = 0.031$, d.f. = 16). There was also a slight decrease (~20%) in the relative fluorescence intensity of the AChR, but this was not significant (paired Student's t-test, $t = 1.48$, $p = 0.159$, d.f. = 16). Only the decrease in AChE at the perlecan-null NMJs was highly significant (paired Student's t-test, $t = 8.02$, $p << 0.0001$, d.f. = 16). Thus, the absence of perlecan does not seem to affect the early events of innervation, including the location of synapse formation on the muscle fiber, the size of the surface areas that form the synapse or the number of fibers that become innervated. This is in contrast to what occurs in agrin-null mice, where nerves fail to terminate properly and continue growing beyond the synaptic region[32].

To determine whether the molecular components of the postsynaptic membrane could accumulate normally in the absence of perlecan, we stained cryostat sections of E18.5 or newborn skeletal muscle muscles for several specific markers for the specialized postsynaptic membrane and synaptic basal lamina. Immunofluorescence studies using antibodies against α-dystroglycan, β-dystroglycan, rapsyn, utrophin and agrin showed that all were present at the NMJs of perlecan-null mice and co-localized with the AChR (Fig. 3). Only perlecan was absent from the synaptic basal lamina (Fig. 3). Thus the absence of perlecan does not seem to affect the localization and organization of the postsynaptic membrane.

We then examined the distribution of AChE in normal and mutant muscles, whole mounts of diaphragms, limb muscles and rib muscles after staining with fluorescent α-Btx and with Oregon Green–conjugated fasciculin 2 (OR–Fas2), a highly specific fluorescent probe for the catalytic subunit of the AChE[26]. AChE co-localized with the AChR in normal heterozygous muscle (Fig. 4a, b, c) but was completely absent from the muscle of perlecan-null mice (Fig. 4d, e, f). Staining of several muscle groups from perlecan-null mice, including front and hind limbs and

Table 1. Quantitation of NMJ sizes and relative AChR and AChE levels in normal and *Hspg2*-null muscles

	AChR		AChE	
	Area (μm²)	Relative fluorescence	Area (μm²)	Relative fluorescence
Wild-type	64.5 ± 6.6	62.7 ± 8.9	48.6 ± 5.6	38.0 ± 5.0
Hspg2 null	85.2 ± 8.7	49.3 ± 4.5	0.6 ± 0.1	0.23 ± 0.07

Data is from thigh muscle fibers (17 each) of 2 normal (wild-type) and 2 perlecan-null E18.5 mice. Surface areas occupied by the NMJs in perlecan-null mice were ~30% larger than those in wild-type mice, with ~20% fewer receptors. In the wild-type mice, the area occupied by AChE at the NMJs was slightly (~25%) lower than that occupied by the receptors in all cases. The relative fluorescence intensity of OR–Fas2 staining (for AChE) at the perlecan-null NMJs was <1% of that at the wild-type NMJs.

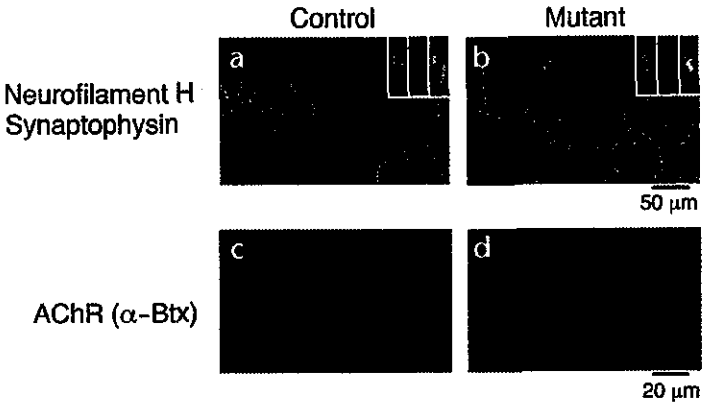

Fig. 2. Muscle fibers of perlecan-null mice are normally innervated. (**a,b**) The occurrence of innervation and the distribution of nerve terminals were examined in E18.5 diaphragm muscles by immunostaining with a combination of antibodies specific for synaptophysin and neurofilament H as a marker for nerve endings and nerve processes. Essentially identical staining patterns for these markers were observed in normal heterozygous control (**a**) and mutant mice (**b**). In both groups of mice, axon bundles ran through the midline of the diaphragms and terminated on synaptic sites on the surfaces of myotubes within 200 μm from the main nerve trunk. Inserts: co-localization of synaptophysin (green) with acetylcholine receptors (α-Btx; red) at sites of nerve–muscle contact; yellow shows areas of overlap. The nerve terminals in mutant mice were always associated with the areas of α-Btx binding and did not extend beyond the borders of the NMJ. Thus, the absence of perlecan did not affect normal distribution of nerve terminals. (**c,d**) Leg muscle fibers from control and mutant mice were labeled with fluorescent α-Btx to visualize NMJs and teased into small bundles to allow individual fibers to be clearly distinguished. In both control (**c**) and mutant mice (**d**), all the fibers seemed to be normally innervated.

diaphragm, all showed a complete absence of the AChE catalytic subunit at the NMJ. Staining for ColQ, the collagen-like tail of AChE, also showed that it was completely absent in the perlecan-null mice (data not shown). However, assays of AChE catalytic activity and of the distribution of oligomeric forms in extracts of heterozygous controls and perlecan-null muscles showed no differences between the two (**Fig. 5**), indicating that the AChE mRNA and protein were normally expressed. The observation that AChR accumulate normally at sites of nerve–muscle contact in perlecan-null muscle also seems to suggest that the mechanisms underlying the accumulation of synapse-specific mRNAs, such as those encoding AChR, were not impaired.

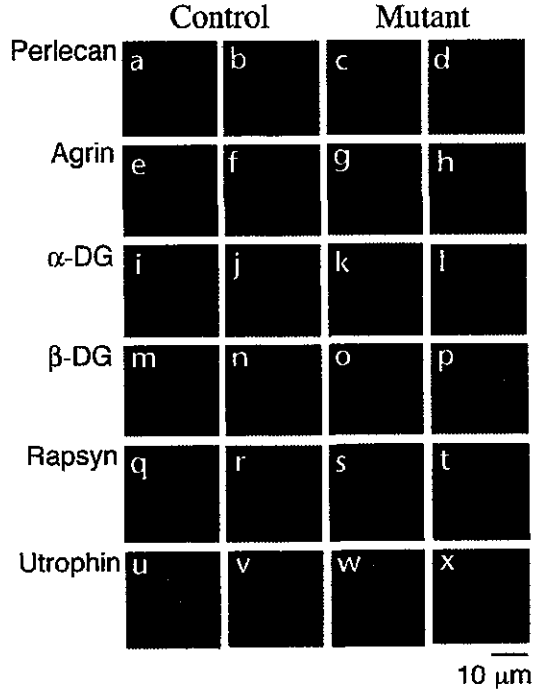

Discussion

From the studies described here, we concluded that perlecan is essential for localizing AChE to the vertebrate NMJ. Although other glycoproteins, such as dystroglycan, agrin and possibly even chondroitin or dermatan sulfate proteoglycans[33–35], at the NMJ might bind AChE, their presence at the NMJs of perlecan-null mice indicates that these alone cannot be responsible for localizing the enzyme to the synapse. On the other hand, as the collagen-tailed form of AChE binds directly to purified perlecan *in vitro*[26] and co-localizes with perlecan and AChR when transplanted onto frozen sections of muscle or tissue-cultured muscle cells[26,27], it is likely that perlecan is the unique acceptor site for AChE at the NMJ. This conclusion is also supported by the observations that perlecan binds to α-dystroglycan[36,37] and that, in the absence of α-dystroglycan in skeletal muscle[38], neither perlecan nor AChE seems to accumulate at the NMJ. In addition,

Fig. 3. The clustering of NMJ-associated molecules is normal in perlecan-null mice. The formation of the NMJ in E18.5 limb muscles was examined using antibodies against identified synaptic molecules plus Alexa-594-conjugated α-Btx to label AChR. At this stage of development, AChR are already well clustered at both normal heterozygous and perlecan-null NMJs. Frozen sections of normal (+/–) and mutant (–/–) mouse limb muscles were stained with fluorescent α-Btx (**b, d, f, h, j, l, n, p, r, t, v** and **x**) and one of several primary antibodies followed by a fluorescent secondary antibody (**a, c, e, g, i, k, m, o, q, s, u** and **w**). Each pair of micrographs shows the same field, viewed under fluorescein optics for the antibody or rhodamine optics for α-Btx, to visualize the acetylcholine receptors. As expected, there is no perlecan immunostaining in the mutant muscle (**c** and **d**), whereas in heterozygotes perlecan is observed in the muscle basement membrane as well as at the NMJ (**a** and **b**). In contrast, agrin, another component of the synaptic basal lamina, was localized normally in both mutant mice (**g** and **h**) and heterozygous controls (**e** and **f**). α-Dystroglycan (α-DG) and β-dystroglycan (β-DG), part of the transmembrane complex that links molecules in the extracellular matrix with components of the myofibrilar apparatus in muscle, were clustered and co-localized with AChR normally in both heterozygous (**i** and **j**; **m** and **n**) and mutant mice (**k** and **l**; **o** and **p**). Rapsyn (**q** and **r**; **s** and **t**) and utrophin (**u** and **v**; **w** and **x**), prominent markers for the crest regions of the postsynaptic junctional folds, were also normally co-localized with AChR at the NMJ of heterozygous control and mutant mice. Thus, the NMJ was formed normally in the perlecan-null mice.

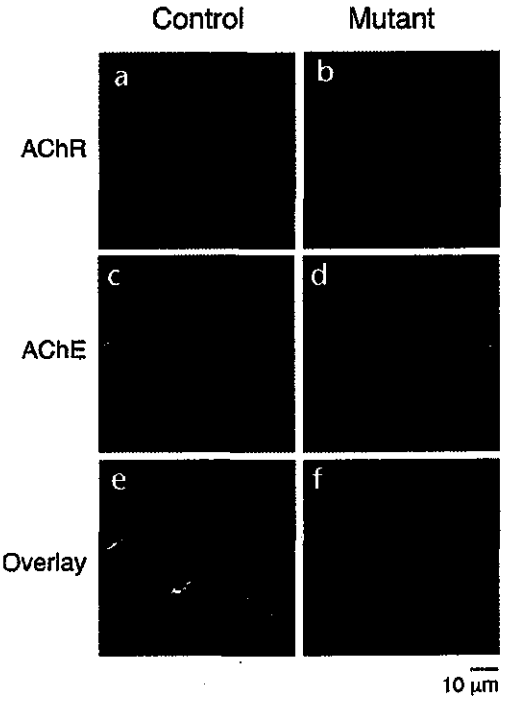

these studies show that, although the highly localized transcription and translation of AChE is necessary to ensure an adequate number of AChE molecules for insertion at the NMJ, ultimately the high-density localization of AChE at the synapse depends entirely on the localization of its binding partner, perlecan. The defect in clustering of AChE at the NMJ of the mutant mice may partially account for the poor movement and respiratory failure of newborn perlecan-null mice.

Two human genetic disorders caused by the perlecan gene have recently been identified: dyssegmental dysplasia, Silverman–Handmaker type (DDSH)[39] and Schwartz–Jampel syndrome (SJS)[40]. DDSH is a neonatal, lethal chondrodysplasia characterized by anisopondyly and micromelia, a phenotype similar to that of perlecan-null mice. DDSH is caused by functional null mutations of the perlecan gene resulting from the fact that truncated perlecan molecules are not secreted into the extracellular matrix. Although abnormality of the NMJ has not been examined in DDSH, we expect a defect in clustering of AChE at the NMJ similar to that in perlecan-null mice. In contrast to those with DDSH, individuals with SJS survive and have a much milder phenotype with chondrodystrophic myotonia. In SJS, truncated perlecan molecules are secreted and present in the basal lamina of muscles (E.A.-H., unpublished data). The number of perlecan molecules is significantly reduced, however, as is the clustering of mutated perlecan and AChE at the NMJ (E.A.-H., unpublished data). Thus, partial impairment of perlecan function causes myotonic myopathy, consistent with our findings that perlecan is crucial for clustering AChE at the NMJ.

Fig. 4. AChE is absent from the NMJs of perlecan-null mice. As the collagen-tailed form of AChE can bind directly to perlecan, and may be the major binding site for AChE at the NMJ[26], we examined the expression of AChE molecules. Whole mounts of embryo limb muscles, as well as intercostal muscle and diaphragm (data not shown), were stained for AChE using fluorescent OR–Fas2 as a probe[26] and for AChR using Alexa-594-conjugated α-bungarotoxin. Although there was strong AChR clustering in both normal heterozygous and perlecan-null muscle, AChE clustering was completely absent from perlecan-null muscle. Thus, perlecan is essential for attachment of the AChE to the synaptic basal lamina.

Methods

Mice. Perlecan-null mice were generated by homologous recombination as previously described; the general phenotype of these mice has been studied in detail[24]. Because the mice die at birth, timed matings between heterozygotes were carried out to generate the homozygous recessive embryos and newborn mice used in the present studies. For most of the studies, E18.5 embryos were used. The animal protocol approved by the NIDCR ACU Committee was used for maintaining and handling mice, and all mice were housed in a mouse facility affiliated with the American Association for the Accreditation of Laboratory Animal Care.

Antibodies. Frozen sections of embryonic limb muscles were incubated with the primary antibody in phosphate-buffered saline containing 10% serum followed by incubation with Alexa-488- or Alexa-594-conjugated secondary antibody. Antibodies against the adult MHC fast and slow isoforms were from Sigma (St. Louis, MO); monoclonal antibody against perlecan domain IV from Chemicon (Temecula, CA); antibody against neurofilament H from Sternberger Monoclonals (Lutherville, MD); antibody against synaptophysin from Zymed (San Francisco, CA); monoclonal antibody against α-dystroglycan (11H6C4) from K. Campbell (U. Iowa, Iowa City); antibody against β-dystroglycan from Novacastra (Newcastle upon Tyne, UK); antibody against rapsyn from S. Froehner (University of Washington, Seattle); antibody against agrin from Z. Hall (University of California, San Francisco); antibody against utrophin from the late K. Arahata (NCPN, Japan); and Alexa-488- and Alexa-594-conjugated goat antibodies against mouse IgG from Molecular Probes (Eugene, Oregon). Whole-mount diaphragms from E18.5 mouse embryos were stained with a mixture of polyclonal rabbit antibodies against neurofilament H (phosphorylated), antibodies against synaptophysin antibodies and Alexa-594-conjugated α-Btx (Molecular Probes), followed by Alexa-488-conjugated secondary antibodies.

Enzyme assays. AChE enzyme activity and oligomeric forms were assessed as previously described[14,15]. Briefly, embryonic limb or diaphragm muscles were homogenized in 10 volumes of extraction buffer

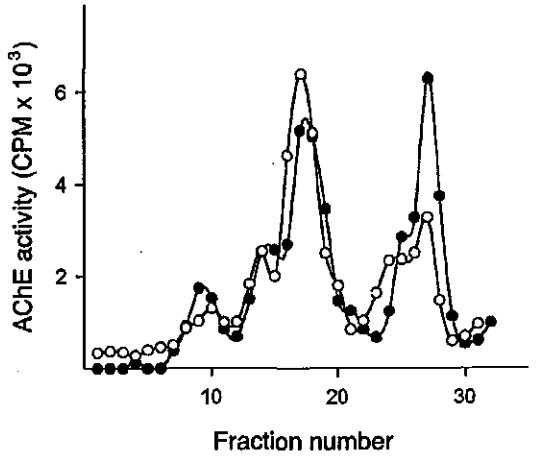

Fig. 5. AChE expression is normal in muscles of perlecan-null mice. Fractions of mouse hind-limb muscle homogenate were assayed for AChE activity using a radiometric method[41] (open circles, wild type; closed circles, *Hspg2* null). The peaks are, from left to right, the A12 collagen-tailed form, the A8 tailed form, and the tetrameric, dimeric and monomeric globular forms. Similar patterns of oligomeric forms were expressed in both wild-type and mutant muscles at approximately the same levels.

consisting of 20 mM sodium borate buffer, pH 9.0, 1 M NaCl, 1.0% Triton X-100, 10 mM EDTA and protease inhibitors. Aliquots were analyzed by velocity sedimentation on 5–20% sucrose gradients and the fractions assayed for AChE activity using a radiometric assay[41]. For quantitative assays (Table 1), mouse thigh muscles were labeled with TRICT–α-Btx and OR–Fas2 and digital images were taken at the two wavelengths appropriate to each dye. Images were calibrated with an optical micrometer and analyzed with Metamorph software.

Acknowledgements

We thank the late K. Arahata as well as J. Sugiyama, M. Dalakas, A. Engel, Z. Hall, S. Froehner, K. Campbell and E. Krejci for generous gifts of antibodies and helpful discussions; H. B. Peng and S. Roper for comments on the manuscript; and J. Quintero for technical assistance. This work was supported by US National Institutes of Health (NIH) intramural funds to Y.Y. and grants from the NIH and Muscular Dystrophy Association to R.L.R.

RECEIVED 21 AUGUST; ACCEPTED 26 DECEMBER 2001

1. Marna, A. & Nachmansohn, D. Choline esterase in voluntary muscle. *J. Physiol (Lond.)* 92, 34–47 (1938).
2. Massoulié, J., Pezzementi, L., Bon, S., Krejci, E. & Vallette, F. M. Molecular and cellular biology of cholinesterases. *Prog. Neurobiol.* 41, 31–91 (1993).
3. Rotundo, R. L. & Fambrough, D. M. Function and molecular structure of acetylcholinesterase. in *Myology* 2nd edn. (eds. Engle, A.E. & Franzini-Armstrong, C.) 607–623 (McGraw-Hill, New York, 1994).
4. Massoulié, J. & Rieger, F. L'Acetylcholinesterase des organes électriques de poissons (Torpille et Gymnote): complexes membranaires. *Eur. J. Biochem.* 11, 441–455 (1969).
5. Hall, Z. Multiple forms of acetylcholinesterase and their distribution in endplate and non endplate regions of rat diaphragm muscle. *J. Neurobiol.* 4, 343–361 (1973).
6. Lwebuga-Mukasa, J. S., Lappi, S. & Taylor, P. Molecular forms of acetylcholinesterase from *Torpedo californica*: their relationship to synaptic membranes. *Biochemistry.* 15, 1425–1434 (1976).
7. Bon, S., Cartaud, J. & Massoulié, J. The dependence of acetylcholinesterase aggregation at low ionic strength upon a polyanionic component. *Eur. J. Biochem.* 85, 1–4 (1978).
8. Vigny, M., Martin, G. R. & Grotendorst, G. R. Interactions of asymmetric forms of acetylcholinesterase with basement membrane components. *J. Biol. Chem.* 25, 8794–8798 (1983).
9. Torres, J. C. & Inestrosa, N. Interaction of heparin with multimolecular aggregates of acetylcholinesterase. *Cell. Mol. Neurobiol.* 5, 303–309 (1985).
10. Feng, G. *et al.* Genetic analysis of collagen Q: roles in acetylcholinesterase and butyrylcholinesterase assembly and in synaptic structure and function. *J. Cell Biol.* 144,1349–1360 (1999).
11. Ohno, K., Brengman, J., Tsujino, A. & Engel, A.G. Human endplate acetylcholinesterase deficiency caused by mutations in the collagen-like tail subunit (ColQ) of the asymmetric enzyme. *Proc. Natl. Acad. Sci. USA* 95, 9654–9659 (1998).
12. Donger, C. *et al.* Mutation in the human acetylcholinesterase-associated collagen gene, ColQ, is responsible for congenital myasthenic syndrome with end-plate acetylcholinesterase deficiency (Type Ic). *Am. J. Hum. Genet.* 63, 967–975 (1998).
13. McMahan, U. J., Sanes, J. R. & Marshall, L. M. Cholinesterase is associated with the basal lamina at the neuromuscular junction. *Nature* 271, 172–174 (1978).
14. Rossi, S. R. & Rotundo, R. L. Localization of "non-extractable" acetylcholinesterase to the vertebrate neuromuscular junction. *J. Biol. Chem.* 268, 19152–19159 (1993).
15. Rossi, S. R. & Rotundo, R. L. Transient interactions between collagen-tailed acetylcholinesterase and sulfated proteoglycans prior to immobilization on the extracellular matrix. *J. Biol. Chem.* 271, 1979–1987 (1996).
16. Jasmin, B. J., Lee, R. K. & Rotundo, R. L. Compartmentalization of acetylcholinesterase mRNA and enzyme at the vertebrate neuromuscular junction. *Neuron* 11, 467–477 (1993).
17. Legay, C., Huchet, M., Massoulié, J. & Changeux, J. P. Developmental regulation of acetylcholinesterase transcripts in the mouse diaphragm: alternative splicing and focalization. *Eur. J. Neurosci.* 7, 1803–1809 (1995).
18. Michel, R. N., Vu, C. Q., Tetzlaff, W. & Jasmin, B. J. Neural regulation of acetylcholinesterase mRNAs at mammalian neuromuscular synapses. *J. Cell Biol.* 127, 1061–1069 (1995).
19. Rossi, S. G. & Rotundo, R. L. Cell surface acetylcholinesterase molecules on multinucleated myotubes are clustered over the nucleus of origin. *J. Cell Biol.* 119, 1657–1667 (1992).
20. Anderson, M. J. & Fambrough, D. M. Aggregates of acetylcholine receptors are associated with plaques of a basal lamina heparan sulfate proteoglycan on the surface of skeletal muscle fibers. *J. Cell Biol.* 97, 1396–1411 (1983).
21. Bayne, E. K., Anderson, M. J. & Fambrough, D. M. Extracellular matrix organization in developing muscle: correlation with acetylcholine receptor aggregates. *J. Cell Biol.* 99, 1486–1501 (1984).
22. Sanes, J. R., Schachner, M. & Covault, J. Expression of several adhesive macromolecules (N-CAM, L1, J1, NILE, uvomorulin, laminin, fibronectin, and a heparan sulfate proteoglycan) in embryonic, adult, and denervated adult skeletal muscle. *J. Cell Biol.* 10, 420–431 (1986).
23. Iozzo, R. V., Cohen, I. R., Grässel, S. & Murdich, A. D. The biology of perlecan: the multifaceted heparan sulfate proteoglycan of basement membranes and pericellular matrices. *Biochem. J.* 302, 625–639 (1994).
24. Arikawa-Hirasawa, E., Watanabe, H., Takami, H., Hassell, J. R. & Yamada, Y. Perlecan is essential for cartilage and cephalic development. *Nat. Genet.* 23, 354–358 (1999).
25. Costell, E. *et al.* Perlecan maintains the integrity of cartilage and some basement membranes. *J. Cell Biol.* 147, 1109–1122 (1999).
26. Peng, H. B., Xie, H., Rossi, S. G. & Rotundo, R. L. Acetylcholinesterase clustering at the neuromuscular junction involves perlecan and dystroglycan. *J. Cell Biol.* 145, 911–921 (1999).
27. Rotundo, R. L., Rossi, S. G. & Anglister, L. Transplantation of quail collagen-tailed acetylcholinesterase molecules on to the frog neuromuscular synapse. *J. Cell Biol.* 136, 367–374 (1997).
28. Bayne, E. K., Anderson, M. J. & Fambrough, D.M. Extracellular matrix organization in developing muscle: correlation with acetylcholine receptor aggregates. *J. Cell Biol.* 99, 1486–1501 (1984).
29. Sanes, J. R., Schachner, M. & Covault, J. Expression of several adhesive macromolecules (N-CAM, L1, NILE, uvomorulin, laminin, fibronectin, and heparan sulfate proteoglycan) in embryonic, adult, and denervated adult skeletal muscle. *J. Cell Biol.* 102, 420–431 (1986).
30. Sanes, J. R. in *Myology* 2nd edn. (eds. Engel, A. G. & Banker, B. Q.) 242–260 (McGraw-Hill, New York, 1994).
31. Leivo, I. & Engvall, E. Merosin, a protein specific for basement membranes of Schwann cells, striated muscle, and trophoblast, is expressed late in nerve and muscle development. *Proc. Natl. Acad. Sci. USA* 85, 1544–1548 (1988).
32. Gautam, M. *et al.* Defective neuromuscular synaptogenesis in agrin-deficient mutant mice. *Cell* 85, 525–535 (1996).
33. Perez-Tur, J., Barat, A., Ramos, M. & Ramirez, G. Chondroitinases release acetylcholinesterase from chick skeletal muscle. *FEBS Lett.* 286, 25–27 (1991).
34. Bowe, M.A., Mendis, D.B. & Fallon, J.R. The small leucine-rich repeat proteoglycan biglycan binds to α-dystroglycan and is upregulated in dystrophic muscle. *J. Cell Biol.* 148, 801–810 (2000).
35. Brandan, E. & Inestrosa, N.C. Co-solubilization of asymmetric acetylcholinesterase and dermatan sulfate proteoglycan from the extracellular matrix of rat skeletal muscles. *FEBS Lett.* 213, 159–163 (1987).
36. Peng, H. B., Ali, A. A., Rauvala, H. J., Hassell, R. & Smalheiser, N. R. The relationship between perlecan and dystroglycan and its implication in the formation of the neuromuscular junction. *Cell Adhes. Comm.* 5, 475–489 (1998).
37. Talts, J. F., Andac, Z., Gohring, W., Brancaccio, A. & Timple, R. Binding of the G domain of laminin α1 and α2 chains and perlecan to heparin, sulfatides, α-dystroglycan and several extracellular matrix proteins. *EMBO J.* 18, 863–870 (1999).
38. Jacobson, C., Côté, P., Rossi, S. G., Rotundo, R. L. & Carbonetto, S. The dystroglycan complex is necessary for stabilization of acetylcholine receptor clusters at neuromuscular junctions and formation of the synaptic basal lamina. *J. Cell Biol.* 152, 435–450 (2001).
39. Arikawa-Hirasawa, E. *et al.* Dyssegmental dysplasia, Silverman–Handmaker type, is caused by functional null mutations of the perlecan gene. *Nat. Genet.* 27, 431–434 (2001).
40. Nicole, S. *et al.* Perlecan, the major proteoglycan of basement membranes, is altered in patients with Schwartz-Jampel syndrome (chondrodystrophic myotonia). *Nat. Genet.* 26, 480–483 (2000).
41. Johnson, C.D. & Russell, R.L. A rapid, simple radiometric assay for cholinesterase, suitable for multiple determinations. *Anal. Biochem.* 64, 229–238 (1975).

Glycoconjugate Journal 19, 263–267, 2003

Role of perlecan in skeletal development and diseases

John Hassell[1], Yoshihiko Yamada[2] and Eri Arikawa-Hirasawa[3]

[1] *The Center for Research in Skeletal Development and Pediatric Orthopaedics, Shriners Hospitals for Children and the Department of Biochemistry and Molecular Biology, College of Medicine, University of South Florida, Tampa, FL 33612, USA,* [2] *The Craniofacial Developmental Biology and Regeneration Branch, National Institute of Dental and Craniofacial Research, NIH, Bethesda, MD 20892, USA,* [3] *Research Institute for Diseases of Old Ages, Juntendo University Medical School, Hongo, Tokyo 113-8421*

Perlecan, a large heparan sulfate proteoglycan (HSPG), is present in the basement membrane and other extracellular matrices. Its protein core is 400 kDa in size and consists of five distinct structural domains. A number of *in vitro* studies suggest multiple functions of perlecan in cell growth and differentiation and tissue organization. Recent studies with gene knockout mice and human diseases revealed critical *in vivo* roles of perlecan in cartilage development and neuromuscular junction activity.
Published in 2003.

Keywords: **heparan sulfate proteoglycan, cartilage development, mutations, chondrodysplasia, myotonia**

Structure and expression

Proteoglycans consist of a core protein containing one or more glycosaminoglycan (GAG) chains. Most proteoglycans have either chondroitin sulfate or heparan sulfate chains or both. Chondroitin sulfate and heparan sulfate are repeating disaccharides of an amino sugar and an uronic acid. The amino sugar is N-acetylgalactosamine in chondroitin sulfate and N-acetylglucosamine in heparan sulfate. The biosynthesis of chondroitin and heparan sulfate is dependent upon a sequence of prior events: transcription of mRNA for a proteoglycan core protein, translation of the mRNA into a precursor protein and assembly of a chain initiation site on the precursor protein. This latter event involves the addition of xylose to certain serine residues on the precursor protein followed by the sequential addition of two galactoses and a glucuronic acid to complete the tetrasaccharide linkage. Linkage region addition is favored on those serines in the precursor protein that are followed by a glycine [1,2]. The synthesis of the GAG then begins with the addition of N-acetylglucosamine, for heparan sulfate, or N-acetylgalactosamine for chondroitin sulfate [3]. The selective addition of N-acetylglucosamine to initiate a heparan sulfate chain is determined by signals in the precursor protein such as the presence of an adjacent cluster of acidic amino acids [4–6]. (Without such signals, the addition of N-acetylgalactosamine would otherwise occur, and a chondroitin sulfate chain would be initiated at that site.) Synthesis of the heparan sulfate chain then occurs by the polymerization of alternating glucuronic acid and N-acetylglucosamine residues by two glycosyltransferases specific for heparan sulfate synthesis [7,8]. Modifying enzymes then introduce sulfate groups at various positions on the growing chain, and some of the glucuronic acid residues are converted to iduronic acid [9].

There are many different genes and gene families for core proteins of heparan sulfate proteoglycans. These include the four members of the syndecan family, the six members of the glypican family, perlecan, agrin and collagen XVIII [9–11]. The syndecan core proteins have a transmembrane segment. The glypicans have a site on the C-terminus of their core proteins that is involved in the formation of a glycosyl phosphatidyl inositol linkage to the plasma membrane. Consequently, both these gene families are considered to be "cell surface proteoglycans." Perlecan, agrin, and collagen XVIII lack these core protein determinants and are thought to be "matrix proteoglycans."

Perlecan is a heparan sulfate-containing proteoglycan that was first discovered in a murine tumor cell line and was shown to be present in all native basement membranes [12]. Subsequent biochemical characterization of murine perlecan showed it contained an estimated 400-kDa core protein with 2–3 heparan sulfate side chains at the N-terminus and one chondroitin sulfate chain at the C-terminus [13,14]. The amino acid sequence of murine perlecan deduced from cDNA cloning [15,16]

To whom correspondence should be addressed: John Hassell, Research Department, Shriners Hospitals for Children—Tampa, 12502 North Pine Drive, Tampa, FL 33612, USA. Tel.: 813-972-2250; Fax: 813-975-7127; E-mail: jhassell@shctampa.usf.edu